Glass Struct. Eng. (2023) 8:119–139
https://doi.org/10.1007/s40940-022-00208-7

RESEARCH PAPER

Structural behaviour and micro-structural characteristics of coloured kilned glass panels

Vlad-Alexandru Silvestru · **Rena Giesecke** · **Benjamin Dillenburger**

Received: 6 July 2022 / Accepted: 4 October 2022 / Published online: 2 November 2022

Abstract In recent years, the architecture, engineering and construction industry is increasingly embracing digital design approaches and robotic production methods. This is as well noticeable in the façade design sector, especially when it comes to architectural design tasks dealing with complex geometries or adaptive components. Although glass is mainly used in facades due to its transparency, it often determines significantly the aesthetic appearance of a building and has to control the transmitted light and the visibility between exterior and interior. Recently, a novel method for producing polychromatic glass panels by fusing granular glass powder of different colours onto the surface of annealed float glass in a kilning process was developed at ETH Zurich. By using a multi-channel tool attached to a robotic arm for placing the granular powder onto the glass surface, digitally designed patterns can be realised precisely and repetitively. This paper focuses on the structural behaviour and the micro-structural characteristics of this novel type of coloured glass panels for façade applications. The bending strength of such glass panels was determined based on four-point-bending tests and was compared to that of annealed float glass. A non-negligible decrease in the bending strength was observed. Furthermore, the reasons for this reduction in structural performance were analysed based on microscopic investigations. It was observed that both the kilning process and the density of deposited granular powder had an influence on the surface microstructure. The presented results are essential for the production of polychromatic kilned glass as well as for future applications of this type of glass panel in façades.

Keywords Coloured kilned glass panel · Four-point bending test · Tensile bending strength · Micro-structural analysis · Glass surface texture · Surface roughness

V.-A. Silvestru (✉)
Institute of Structural Engineering, ETH Zurich,
Stefano-Franscini-Platz 5, 8093 Zurich, Switzerland
e-mail: silvestru@ibk.baug.ethz.ch

R. Giesecke · B. Dillenburger
Institute of Technology in Architecture, ETH Zurich,
Stefano-Franscini-Platz 1, 8093 Zurich, Switzerland

1 Introduction

Digital design approaches and automatized robotic production methods enjoyed increasing interest from the architecture, engineering and construction (AEC) industry in recent years. However, while for materials like concrete and steel, various research projects were conducted and some representative construction projects were completed, in the case of glass, such approaches and production methods are rather limited. First attempts of using additive manufacturing (AM) for glass at an architectural scale were done by Inamura et al. (2018) in the form of glass columns or by Seel et al. (2018) in the form of prototypical connections. Whereas these projects focused on realizing structural components made of glass, digital design approaches

Fig. 1 Views of the pavilion with polychromatic kilned glass panels showing (**a**) the relationship to the surroundings through the decorative pattern applied and (**b**) the graded transparency obtained through the colour grading process. Images credit: Digital Building Technologies, ETH Zurich; Photographer: Evangelos Roditis

and robotic production methods were applied recently also for achieving novel architectural glass products. Giesecke and Dillenburger (2022) and Giesecke et al. (2022) developed a method for large-scale robotic fabrication of polychromatic glass by fusing granular glass powder on annealed float glass panels. An application of this type of glass for a mock-up pavilion built in 2021 is shown in Fig. 1. As it is the case of other processing technologies of glass, understanding the material behaviour at different temperatures in the transition range from melt to solid is of ultimate importance for applying additive manufacturing principles to glass.

The glass mostly used in the AEC industry, soda-lime silicate glass, has a glass transition temperature of around 570 °C, a softening point of around 725 °C and a working point of around 1030 °C (Schneider et al. 2016). In addition, the strain point is situated at around 505 °C, while the annealing point is at approximately 550 °C. These temperatures and the related changing viscosities of the glass are used in various processing steps, including tempering, shaping or surface treatments. For thermal tempering, the annealed float glass is heated to approximately 100 °C above the glass transition temperature, where it is in a viscoelastic state, and subsequently it is quenched from both sides. This allows to obtain a structurally favourable residual stress state. In case of hot-bending, the flat glass is heated as well to approximately 100 °C above the glass transition temperature to reach a viscosity, which allows the glass either to slump in a mould due to gravity or to be formed by movable moulds.

Several decorative surface treatment processes are available nowadays, ranging from (i) patterned glass (see EN 572-5 2012) done by casting through patterned rollers, over (ii) enamelled glass done by burning a ceramic frit colour into the annealed glass during the tempering process, to (iii) digital printing methods done by applying ceramic or organic colours on the glass surfaces. All these processes show certain disadvantages. For instance, patterned glass and enamelled glass lead to reduced bending strengths and are either translucent or opaque. Enamelled glass shows limitations in the achievable colours compared to digital prints on glass surfaces, which allow for photo-realistic images. Digital prints on glass surfaces exhibit a lower durability compared to enamelled glass. From the available decorative surface treatment processes, only the enamelling requires the glass to be reheated. Maniatis and Elstner (2016) conducted investigations on the structural behaviour of enamelled glass.

A decorative surface treatment by fusing coloured powder on flat glass was used by Saint Gobain Glass Solutions in collaboration with TNO for the facades of the Dutch Institute of Sound and Vision in Hilversum (see TNO 2007). Granules in three basic colours were deposited in a patterned mould and fused with the glass sheets at temperatures of around 800 °C.

While for fusing the ceramic frit into the glass, temperatures slightly below the softening point are sufficient, for a proper mixing of glass coming from different recycled cullet, higher temperatures are necessary. Bristogianni et al. (2020) and Bristogianni et al. (2021) used temperatures between 820 and 1120 °C to kiln-cast small-scale beams (30 × 30 × 240 mm) from cullet coming from different previous applications. Related to cast glass, Oikonomopoulou et al. (2018) showed that the material used for the moulds influenced the obtained finishing surface. While permanent stainless steel or graphite moulds allowed for glossy finishes, silica plaster and alumina-silica plaster lead to translucent and rough finishes. To restore transparency and to increase accuracy of cast glass, generally, grinding and polishing were required when using the latter mould types in past applications.

In contrast to the above methods, polychromatic kilned glass allows for an enhanced diversity enabled by digitally designed multi-colour patterns that can be realized in a precisely controlled and repeatable manner thanks to the robotic dispensing of the colour. However, the structural performance of this glass type has not been addressed yet, limiting its application. Therefore, this research investigates the structural behaviour and the micro-structural characteristics of coloured kilned glass panels. The panels were produced in a similar manner to the polychromatic glass presented by Giesecke and Dillenburger (2022) and by Giesecke et al. (2022).

2 Materials and methods

This section briefly describes the materials involved in the presented investigations and provides information on the applied methodology for producing the coloured kilned glass panels, for determining their structural behaviour and for evaluating their micro-structural characteristics.

2.1 Material properties of the glass panels and the granulate

Annealed float glass as regulated in EN 572-1 (2016) and EN 572-2 (2012), with a nominal thickness of 8 mm was used for the panels investigated in this paper (PLANICLEAR® from Saint-Gobain without any additional coatings). This basic product made from soda-lime silicate glass is the one mostly used in facades, often further processed to thermally tempered glass, laminated glass or insulating glass units. From a mechanical point of view, EN 572-1 (2016) specifies for annealed soda-lime silicate glass a characteristic bending strength of 45 MPa and a Young's modulus of 70′000 MPa. The thermal expansion coefficient of such glass is 9×10^{-6} K^{-1}.

For colouring the annealed float glass panels by fusing, granulate powder from OPTUL Spezialglas GmbH was used. Powder granules of the transparent colour FF-BF 0076 Chrome Green with grain sizes between 0.36 and 1.00 mm were used in the experiments discussed in this paper. For the pavilion in Fig. 1, other colours, like FF-BF 0078 Dark Green, FF-BF 2135 Yellow, and FF-BF 3100 White were used as well (Giesecke et al. 2022; Giesecke and Dillenburger 2022). These granular glass powders were developed to match the thermal expansion coefficient of annealed float glass to enable fusing without breakage, according to OPTUL Spezialglas GmbH. The specified thermal expansion coefficient of 8.2 (± 0.3) × 10^{-6} K^{-1}, however, is slightly lower than that of soda-lime silicate glass and could eventually lead to residual stresses after the fusing and kilning process. A colour palette of 40 compatible granular glass colours, both transparent and opaque, are available. The granules come in six different sizes ranging from powder of 0.00–0.36 mm up to chips of 5.00–8.50 mm (OPTUL Float 2022). This wide range of available colours and grain sizes opens up a vast diversity of potentially achievable design patterns and resolutions. Due to the packing of the granules, it is not only possible to add two-dimensional properties to the glass, but also three-dimensional relief features (Giesecke and Dillenburger 2022).

2.2 Manufacturing of polychromatic kilned glass panels

The polychromatic patterns of the glass panels for the pavilion shown in Fig. 1 were digitally designed to visually interact with the surroundings. For the robotic dispensing process, granular glass of four colours was placed in a multi-channel tool attached to a robotic arm or motion system, as shown in Fig. 2a (Giesecke et al. 2022; Giesecke and Dillenburger 2022). The robotic

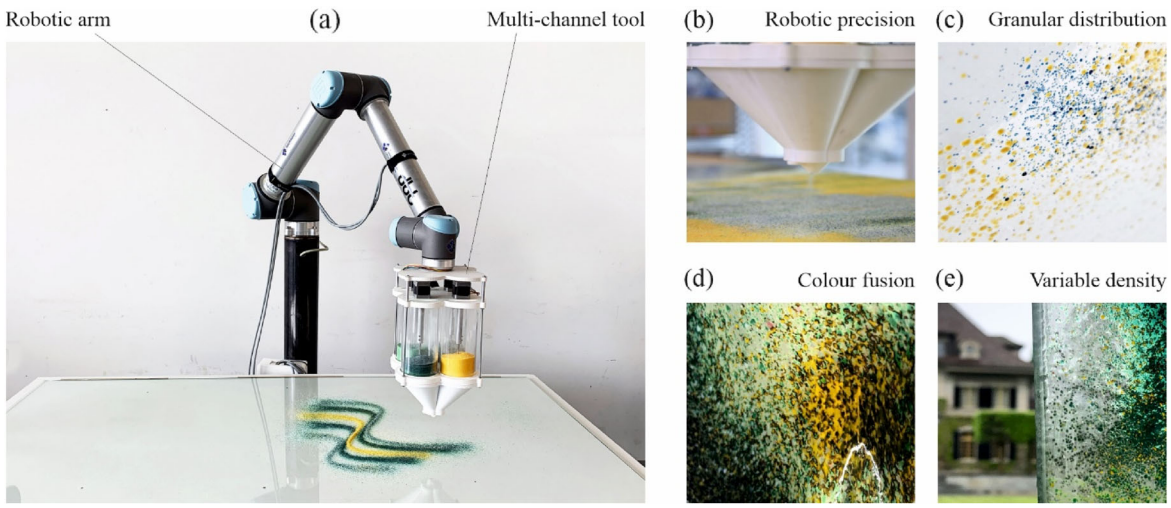

Fig. 2 Multi-channel tool setup for robotic application of the coloured granules (**a**), and different features of the achievable colour patterns: (**b**) repeatability due to robotic precision, (**c**) granular distribution, (**d**) dense colour fusion and (**e**) variable transition between colour densities. Images credit: Digital Building Technologies, ETH Zurich

arm moved along a specific toolpath based on the pattern designed and dispensed a controlled volume of material on the air side of the annealed float glass panels. The granules could also be distributed manually, as it was done for the panels investigated in this paper from a structural and micro-structural point of view. However, the robotic process enabled the precise, repetitive inscription of decorative and functional (e.g. light and view control) material patterns, as well as continuity of patterns between elements without the use of a template through a digital design-to-production workflow. For the investigations within this paper, a manual dispensing procedure was chosen for obtaining random patterns. The granulate powder was distributed directly on the glass surface, without using a fusing gel. Both the robotic dispensing process and the manual dispensing process lead to similar varied colour distributions, ranging from isolated granular patterns to densely coloured areas (see Fig. 2c–e).

For the kilning process, the annealed float glass panels with the granular glass deposited on top (on the air side) were placed in a Nabertherm GF600 kiln (see Fig. 3a), which could host glass panels with dimensions of up to 1 m × 2 m. A textile layer made of a 2 mm thick ceramic fibre paper was used as a substratum for the glass panels. For the kilning process, the glass panels were heated to 800 °C and cooled in a controlled annealing process according to the temperature vs. time curve shown in Fig. 3b. The temperature of 800 °C was chosen based on the fact that at this temperature the fused coloured granulate powder develops the desired nuances.

2.3 Four-point bending tests

To assess the structural performance of the novel polychromatic/coloured kilned glass panels in comparison to standard annealed float glass panels, a series of four-point-bending tests were conducted. The test specimens and the test setup were designed according to EN 1288-3 (2000). The four-point-bending test setup, which includes the influence of the free glass edges on the bending strength, was preferred to a coaxial double ring test setup, since the strength values determined in these investigations should characterize the glass panels with free edges used for the pavilion shown in Fig. 1. The main dimensions of the test specimens and the test setup are provided in Fig. 4a, while Fig. 4b shows the assembled test setup. A total of twelve specimens were tested, as listed in Table 1. This number of specimens is not sufficient for statistically significant results, but allows to provide first information on the mechanical properties of the coloured kilned glass panels compared to the annealed float glass panels. According to existing standards, no differentiation in strength is made for annealed float glass depending on whether the tin side or the air side is subjected to tension. For the coloured

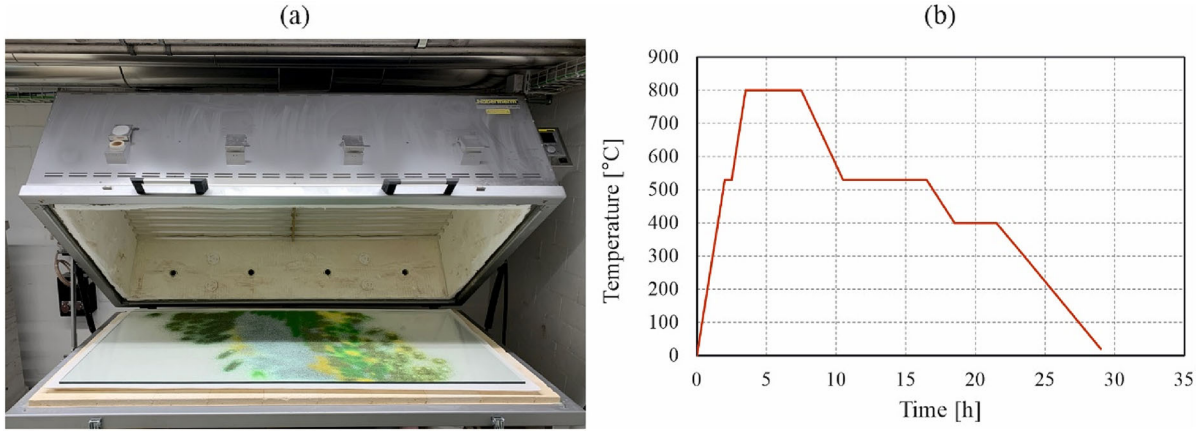

Fig. 3 Nabertherm GF600 glass kiln for fusing the granules into the float glass surface (**a**) and applied temperature curve for producing the investigated coloured kilned glass panels (**b**)

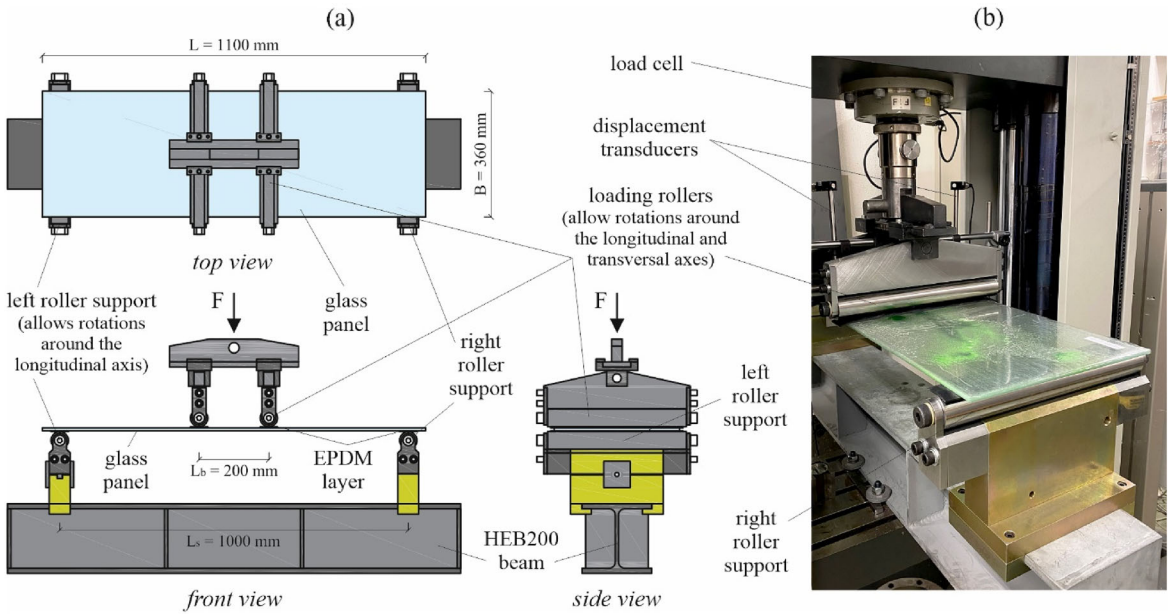

Fig. 4 Schematic illustration of the geometry of the test setup with built-in specimen (**a**) and test setup with its components during testing of a coloured kilned glass panel (**b**)

kilned glass, it was expected that the air side, on which the green granular powder was dispensed and fused, and the tin side, which was in contact with a textile during the kilning process, might have suffered different structural changes. Thus, specimens of the kilned glass panels were tested both with the coloured air side and with the tin side, respectively, subjected to tension.

The glass panels had nominal dimensions of 1100 mm in length, 360 mm in width and 8 mm in thickness. The length and the width were chosen according to EN 1288-3 (2000), while the thickness was the same as for the panels in the pavilion mentioned in the introduction. Especially for the kilned glass panels, deviations from these nominal dimensions were expected. Therefore, before testing, the actual sizes of each specimen were measured at four positions for the

Table 1 Overview of the performed four-point-bending test series

Specimen type	Number of specimens	Specimen nomenclature
Reference annealed float glass panels with tin side under tension	4 specimens	TS-01-FG-ref | TS-02-FG-ref TS-03-FG-ref | TS-04-FG-ref
Coloured kilned glass panels with coloured side under compression	4 specimens	TS-05-KG-tin | TS-06-KG-tin TS-07-KG-tin | TS-08-KG-tin
Coloured kilned glass panels with coloured side under tension	4 specimens	TS-09-KG-air | TS-10-KG-air TS-11-KG-air | TS-12-KG-air

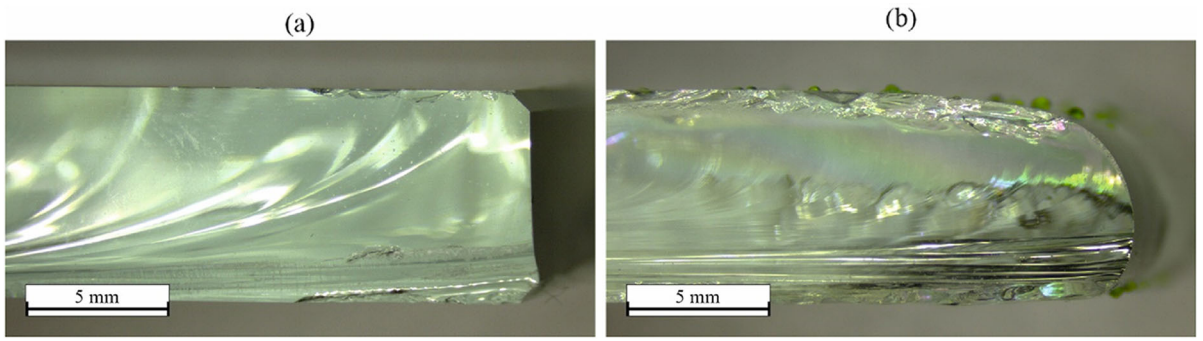

Fig. 5 Representative edge shapes of the reference annealed float glass panels (**a**) and the coloured kilned glass panels (**b**)—pictures of resulting shards after completing the four-point-bending tests

width and at eight positions for the thickness. The reference annealed float glass panels had polished edges (see Fig. 5a). The coloured kilned glass panels, for which float glass with cut edges was used, had after the kilning process rounded nearly quadrant-shaped edges (see Fig. 5b). For the kilned glass panels, the thickness measurements were conducted as far away from the edges as the calliper allowed, to exclude the thinner areas at the edges; these measurements included both zones without and zones with granules, since it was not possible to completely avoid measurement points with granules. Before testing, a 0.03 mm thin polypropylene (PP) self-adhesive film was applied on the top side of each panel (side under compression during testing) to allow an easier removal of the broken specimens and a better evaluation of the failure patterns after testing.

The tests were performed under load control on a Zwick universal testing machine. The load was applied with a load rate of 38.4 N/s, which corresponds for the given cross-section of the panels to a stress rate of 2 MPa/s, as specified in EN 1288-3 (2000). The glass panels were simply supported on rollers at both ends. The distance between the supports was $L_s = 1000$ mm. The load was applied as well with rollers positioned at a distance of $L_b = 200$ mm to each other. Soft layers of 3 mm thin ethylene-propylene-diene-monomer (EPDM) were applied between all the steel rollers and the glass panels to avoid stress concentrations.

In addition to the acting force and the machine displacement, the vertical deflection of the panels at midspan was measured near each of the two longitudinal bended edges with linear variable differential transformers (LVDTs), as shown in Fig. 4b. Beside evaluating load vs. displacement curves and fracture patterns, the equivalent bending strength $\sigma_{b,eq,B}$ was determined for the different specimens with Eq. (1) according to EN 1288-3 (2000).

$$\sigma_{b,eq,B} = k \cdot \left[F_{\max} \cdot \frac{3 \cdot (L_s - L_b)}{2 \cdot B \cdot h^2} + \sigma_{b,eq,G} \right] \quad (1)$$

Here, the factor $k = 1.0$ was used, since both specimens for which the fracture initiated on the surface and such for which the fracture initiated at the edge were considered. F_{max} was the maximum force measured with the load cell, B was the measured average width of the specimens and h the measured average thickness of the specimens. The equivalent bending strength resulting

from the self-weight of the glass panels $\sigma_{b,eq,G}$ was determined with Eq. (2).

$$\sigma_{b,eq,G} = \frac{3 \cdot \rho \cdot g \cdot L_s^2}{4 \cdot h} \tag{2}$$

Here, the density of glass $\rho = 2'500$ kg/m^3 and the gravitational acceleration $g = 9.81$ m/s^2 were used. The bending strengths were determined as equivalent values, since for the kilned glass the thickness was less uniform due to the production process, similar to patterned glass. Furthermore, the Young's modulus of the glass E was estimated from the obtained measurements for the different glass panels with Eq. (3), where $y = 4$ mm was chosen as the vertical deflection in the middle of the panels and $F_{(y\,=\,4\text{ mm})}$ was the force recorded at this displacement.

$$E = \frac{3 \cdot F_{(y=4\text{ mm})}}{4 \cdot y \cdot B \cdot h^3} \cdot \left(\frac{L_s^3}{3} + \frac{L_b^3}{6} - \frac{L_s \cdot L_b^2}{2} \right) \tag{3}$$

2.4 Microscopic investigations of glass surfaces

The production process for the coloured kilned glass included the fusion of the dispensed granules into the air surface of the annealed float glass panels. Furthermore, the glass panels were positioned with the tin surface on a textile during the kilning process. Modifications, which might have influenced the bending strength, were expected for both of the surfaces on micro-structural level. For evaluating these modifications and eventual damages of the glass surfaces through the production process, microscopic investigations were carried out on shards resulting after performing the four-point-bending tests. The shards were cleaned with pressurized air and wiped over with a cloth with acetone. In a first step, a stereo light microscope Leica M60 able to zoom between 6.3X and 40X was used. Two levels of magnitude (10X and 40X) were used to observe micro-structural differences on the two surfaces of the coloured kilned glass panels compared to the reference annealed float glass panels. The characteristics and the size of observed features were analysed. For the coloured side of the kilned glass panels, an additional differentiation was made depending on the density of the dispensed and fused granulate.

In a second step, a confocal laser microscope Zeiss LSM 780 upright was used to characterise the surface condition in terms of texture and roughness. This method allowed to capture sharp images of a defined plane of focus, without disturbing light from the background or other regions of the specimen. By stacking several such images, the three-dimensional texture of surfaces could be analysed in detail. For the investigated glass surfaces a Fluar 5X/0.25 objective and a laser with a wavelength of 405 nm were used. The obtained images had dimensions of 2.83 mm × 2.83 mm with a resolution of 4096 pixel × 4096 pixel.

For the results presented in Sect. 3.4, a representative area of 2.0 mm × 2.0 mm was evaluated for (i) the air side and (ii) the tin side of the reference annealed float glass, for (iii) the uncoloured side of the kilned glass and for the coloured side of the kilned glass, with (iv) low, (v) medium and (vi) high density of the dispensed and fused granulate. Based on these areas, the local waviness and roughness of the surfaces were evaluated along a chosen representative profile in order to allow a quantitative comparison of the surfaces. Furthermore, 3D diagrams of a magnified area of 0.5 mm × 0.5 mm were plotted to illustrate the different textures of the reference annealed float glass surfaces and the kilned glass surfaces. For evaluating the roughness, first, the low frequencies (waviness) and the high frequencies (roughness) were separated from each other by applying a Gaussian filter with a cut-off of 0.25 mm. Three different characteristic roughness values were calculated from the profiles according to EN ISO 4287 (2010):

- The arithmetic mean deviation of the roughness profile R_a, calculated as the average vertical distance of each measured point from the mean profile line along the evaluation length of 2.0 mm;
- The maximum height of the roughness profile R_z, calculated as the average of maximum peak-to-valley distances from a defined number of sampling lengths (five such lengths of 0.4 mm each were used);
- The maximum valley depth of the roughness profile R_v, calculated as the vertical distance between the lowest measured point along the evaluation length and the mean profile line.

While the first two values are often provided when characterizing surfaces, the latter one was considered as

a rough indicator for the depth of strength determining surface features, e.g. cracks.

3 Results and discussion

The results obtained from the different four-point-bending test series were analysed and compared to each other from a structural point of view in a first step. Afterwards, findings from micro-structural analyses of the surfaces were evaluated and related to the structural performance of the different glass panels.

3.1 Four-point-bending test results

The glass panels tested under four-point-bending in the different series exhibited significant differences regarding their structural performance. Based on the force vs. displacement curves plotted in Fig. 6, it can be observed that the kilning process applied to obtain the coloured glass panels had a degrading effect on the mechanical performance. A linear development of the curves with similar gradients was observed for all specimens, as it is usual for the linear-elastic material glass. However, in terms of failure loads and maximum mid-span deflections, the kilned glass panels with the coloured side under compression (Fig. 6b) and those with the coloured side under tension (Fig. 6c) reached on average only around two thirds and less than half, respectively, of the values achieved for the reference annealed float glass panels (Fig. 6a). This suggested that the fusing of the granular powder on the air side lead to significant micro-structural deterioration of the surface, while the positioning of the glass panels on the textile during the kilning process resulted as well in non-negligible surface modifications.

For a better comparison of the four-point-bending test results and their scatter, numerical values for each test as well as average values and coefficients of variation are provided in Table 2 for the reference annealed float glass panels, in Table 3 for the kilned glass panels with the coloured side under compression and in Table 4 for the kilned glass panels with the coloured side under tension. Beside the maximum force and the maximum deflection, the tables include the measured glass panel widths and thicknesses as well as the calculated maximum bending stresses and the Young's moduli. Despite the small number of test specimens per test series, especially for the material glass which shows a large scatter of mechanical properties, the provided values allowed a good assessment of the range of values for the different parameters.

In the case of the dimensions, it was observed that the width of the panels increased after the kilning process. This was in agreement with the reshaped edge geometry and confirmed the softening of the material at the targeted temperature of 800 °C. Based on the measured thickness values, it seemed that the thickness was increased after the kilning process. In reality, the thickness of the kilned glass depended on the local distribution and amount of the dispensed granular powder and the degree to which the powder fused with the glass (see also microscopic images in Sects. 3.3 and 3.4). This explained also the higher scatter of the thickness in case of the coloured kilned glass compared to the annealed float glass.

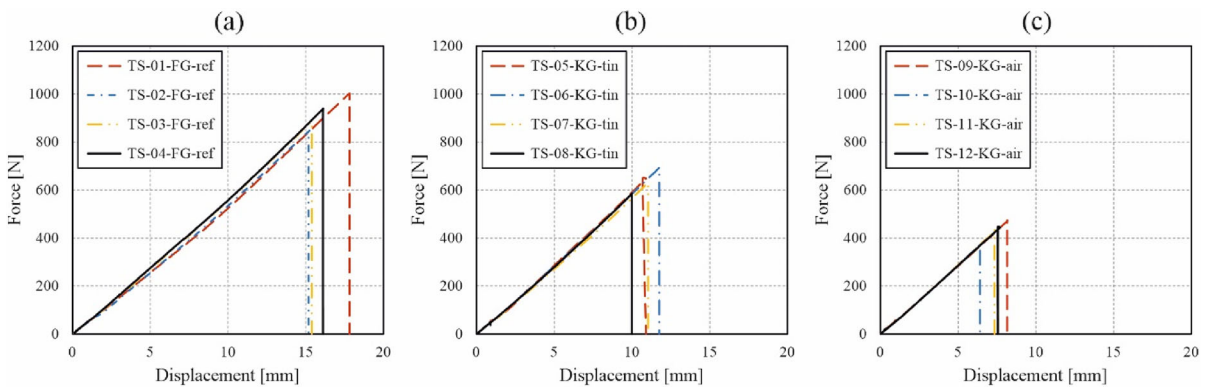

Fig. 6 Force vs. displacement curves for the reference annealed float glass panels (**a**), for the coloured kilned glass panels with the coloured side under compression (**b**) and with the coloured side under tension (**c**)

Table 2 Measured cross-section dimensions and mechanical properties determined from the four-point-bending tests for the reference annealed float glass panels

Specimen	Panel width[a] (mm)	Panel thickness[a] (mm)	Maximum force (N)	Maximum deflection (mm)	Maximum stress (MPa)	Young's modulus (MPa)
TS-01-FG-ref	359.7	7.84	1′002.6	17.81	56.8	69′197
TS-02-FG-ref	359.4	7.83	847.7	15.23	48.5	68′847
TS-03-FG-ref	359.5	7.88	882.6	15.38	49.8	71′392
TS-04-FG-ref	359.5	7.85	939.8	16.11	53.3	74′059
Average	359.5	7.85	918.2	16.13	52.1	70′874
Coefficient of variation	0.1%	0.30%	7.4%	7.32%	7.1%	3.4%

[a]The provided dimensions are averages of four different values for the width and eight different values for the thickness. For the determination of the coefficient of variation all the measured dimension values were used

Table 3 Measured cross-section dimensions and mechanical properties determined from the four-point-bending tests for the coloured kilned glass panels with the coloured side under compression

Specimen	Panel width[a] (mm)	Panel thickness[a] (mm)	Maximum force (N)	Maximum deflection (mm)	Maximum stress (MPa)	Young's modulus (MPa)
TS-05-KG-tin	362.6	8.19	647.9	10.90	35.9	71′667
TS-06-KG-tin	362.4	8.29	694.2	11.77	37.6	69′281
TS-07-KG-tin	362.1	8.44	630.8	11.04	33.9	64′898
TS-08-KG-tin	362.4	8.01	586.1	10.01	33.1	71′483
Average	362.4	8.23	639.7	10.93	35.1	69′332
Coefficient of variation	0.2%	3.23%	7.0%	6.61%	5.7%	4.5%

[a]The provided dimensions are averages of four different values for the width and eight different values for the thickness. For the determination of the coefficient of variation all the measured dimension values were used

Table 4 Measured cross-section dimensions and mechanical properties determined from the four-point-bending tests for the coloured kilned glass panels with the coloured side under tension

Specimen	Panel width[a] (mm)	Panel thickness[a] (mm)	Maximum force (N)	Maximum deflection (mm)	Maximum stress (MPa)	Young's modulus (MPa)
TS-09-KG-air	361.9	8.16	473.2	8.18	26.8	71′919
TS-10-KG-air	362.5	8.10	373.4	6.42	21.7	72′058
TS-11-KG-air	362.2	8.00	432.8	7.42	24.9	73′697
TS-12-KG-air	362.3	7.99	445.6	7.69	25.8	73′920
Average	362.2	8.06	431.3	7.43	24.8	72′899
Coefficient of variation	0.2%	2.41%	9.8%	10.03%	9.0%	1.4%

[a]The provided dimensions are averages of four different values for the width and eight different values for the thickness. For the determination of the coefficient of variation all the measured dimension values were used

As already observed from the force vs. displacement curves, the maximum force, maximum deflection and maximum stress values in Tables 2, 3 and 4 show that the kilned glass panels behave worse than the reference annealed glass panels from a structural point-of-view. The lower reached values could be explained based on modifications suffered by the surfaces as a consequence of the kilning process, which were observed in the microscopic analyses presented in Sects. 3.3 and 3.4. The scatter of the force, deflection and stress values evaluated as coefficients of variation was similar for the reference annealed glass panels and the kilned glass panels with the coloured side under compression (around 6–7%) and a little higher for the kilned glass panels with the coloured side under tension (around 9–10%). This slightly higher scatter was attributed to the non-uniformly distributed granulate powder and the observed devitrification, which lead to a more roughened glass surface with defects of more diverse magnitude, as exemplified in Sect. 3.4. In terms of calculated bending stresses, the values for the reference annealed float glass panels were a little higher than the characteristic bending strength value of 45 MPa generally provided in standards with an average value of around 52 MPa. The lower average bending stress values calculated for the kilned glass panels of around 35 MPa with the coloured side under compression and of around 25 MPa with the coloured side under tension were in the range of bending strength values found in literature for patterned glass (e.g. Haldimann et al. 2008; Schneider et al. 2016). The estimated Young's modulus values were for all specimens in the range of the value of 70′000 MPa found in literature. However, no significant influence of the kilning and fusing processes on the Young's modulus was observed. The slightly different Young's modulus values determined for the kilned glass panels were with high probability due to the larger scatter of the average thickness values, determined from measurements at points both with and without powder granules.

3.2 Fracture patterns of the different glass panels

The fracture pattern of a glass type is relevant for assessing the risk of injury in case of breakage as well as for the residual load-bearing capacity in case of combination to laminated glass. Furthermore, the position of the fracture initiation on the surface or at the edge allows to estimate whether the edge bending strength is lower than the overall bending strength. In the case of the tested reference annealed float glass panels, which had polished edges, for three specimens the fracture initiated on the glass surface (see Fig. 7a–c), while for one specimen it initiated at the glass edge (see Fig. 7d). This indicated that, as expected, the polishing reduced pronounced flaws at the edges and that the edge bending strength was not lower than the overall bending strength.

For the kilned glass panels tested with the coloured side under compression, the crack always initiated from the edge (see Fig. 7e–h), while for those tested with the coloured side under tension always on the surface (see Fig. 7i–l). The initiation from the edge could be explained by the fact that the kilned glass panels were thinner in the edge areas due to the nearly quadrant-shaped geometry. Moreover, the lower sides of the cut edges, which were in contact with the textile during kilning and subjected to tensile stresses during the testing, might still have exhibited some residual damages after kilning. The crack initiation on the surface in the case of the panels with the coloured side under tension indicated that the fused granular powder had a significant influence on the near-surface micro-structure and implicitly on the bending strength. The location of failure initiation was with high probability determined by the unevenness of the kilned glass panels combined with surface damages caused by the non-uniformly distributed fused granules.

The main fan-shaped cracks are highlighted in the images from Fig. 7. It was observed that for almost all specimens the fracture initiated between the loading rollers. Only for two of the kilned glass panels with the coloured side under tension, the fracture initiated slightly outside the loading rollers, indicating damages of the surface through the fused granular powder. The cracks in Fig. 7, which are not highlighted, resulted when the already fractured specimens hit the test setup and were therefore not considered for the evaluation in this section.

When comparing the fracture patterns of the different series to each other, it was observed that the reference annealed glass panels and the kilned glass panels tested with the coloured side under compression

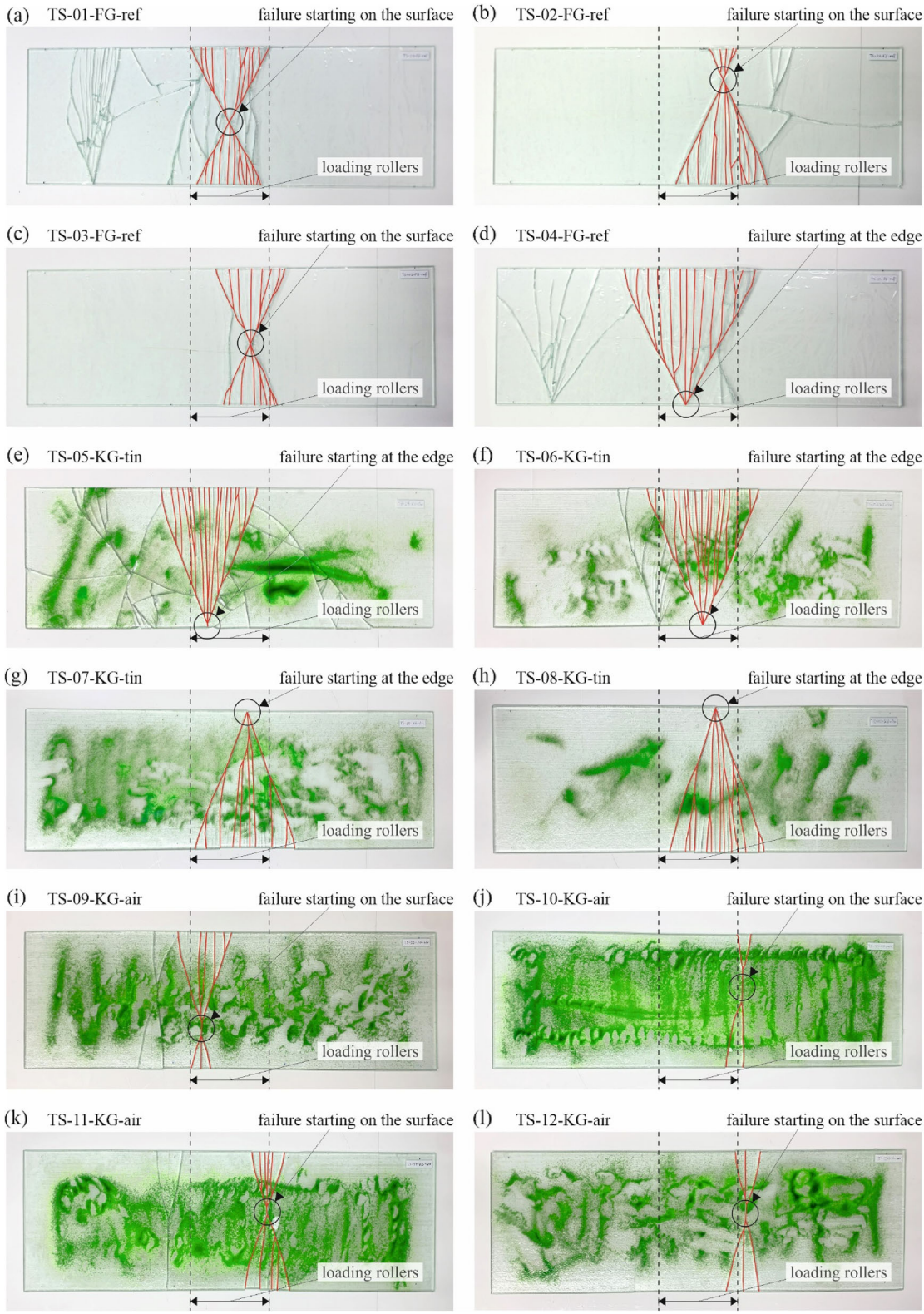

Fig. 7 Fracture patterns for the reference annealed float glass panels (**a–d**) and for the coloured kilned glass panels with the coloured side under compression (**e–h**) and with the coloured side under tension (**i–l**)

exhibited patterns of similar complexity, with multiple cracks distributed in the shape of a fan. The fracture patterns of the kilned glass panels tested with the coloured side under tension, however, were much simpler, with only a low number of cracks. Moreover, for the reference annealed glass panels with crack initiation in the surface, the fan-shaped cracks intersect in one point, while for the kilned glass panels tested with the coloured side under tension, a crack parallel to the shorter glass panel edges was observed, from which a few further cracks developed towards the longer glass panel edges. The limited fragmentation observed for the kilned glass panels tested with the coloured side under tension indicated a lower bending strength of these samples, which was in agreement with the determined strength values provided in Sect. 3.1.

When assessing the safety and the risk of injury in case of breakage of monolithic glass panels, the size and sharpness of the resulting shards is relevant. While annealed glass, whose fracture pattern exhibits radial cracks and large, sharp fragments, is considered to present a high risk of injury, fully tempered glass with net-like cracks and small, dice-shaped, less sharp fragments presents a lower risk. In case of the tested kilned glass panels, the resulted shards exhibited similar characteristics in terms of size and sharpness to those obtained from the annealed glass panels. Based on the large, sharp fragments, the same qualitative risk of injury can be assumed for the coloured kilned glass as for the reference annealed glass.

3.3 Analysis of surfaces from the different glass panel types based on stereo microscope images

For explaining the worse performance of the coloured kilned glass panels in the four-point-bending tests compared to the reference annealed float glass panels, the different surfaces were analysed under a stereo microscope. The lower zoom factor of 10X was used to get an overview of the surface characteristics, while the higher zoom factor of 40X allowed the identification and assessment of specific features. Figure 8 shows a representative area of a reference annealed glass panel near a broken edge. Significant visible features or defects (except those resulted due to the fracture in direct vicinity of the edge) could not be observed, neither with the lower zoom factor, nor with the higher one.

In contrast with the reference annealed float glass panels, both the uncoloured and the coloured sides of the kilned glass panels exhibited features that could be associated with the earlier failure in the bending tests. In case of the uncoloured side, bubbles of different sizes distributed all over the surfaces could be observed, as shown in Fig. 9a. A closer evaluation with the higher zoom factor (see Fig. 9b) allowed to measure the size of the bubbles, which ranged from a few micrometres to around half of a millimetre in diameter. Most of the bubbles had diameters of less than 400 μm and could be categorized as seeds, while some few were slightly larger and could be classified as blisters. Part of the bubbles were entirely sunken under the glass surface, while others were directly on the surface, as the one shown

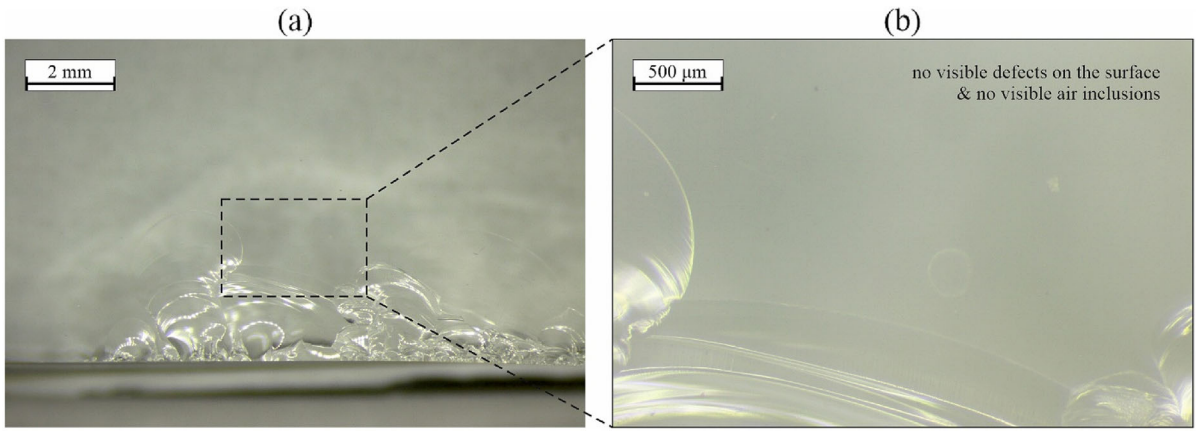

Fig. 8 Air side of the reference annealed float glass panels—representative stereo microscope images obtained with zoom factors of 10X (**a**) and 40X (**b**)

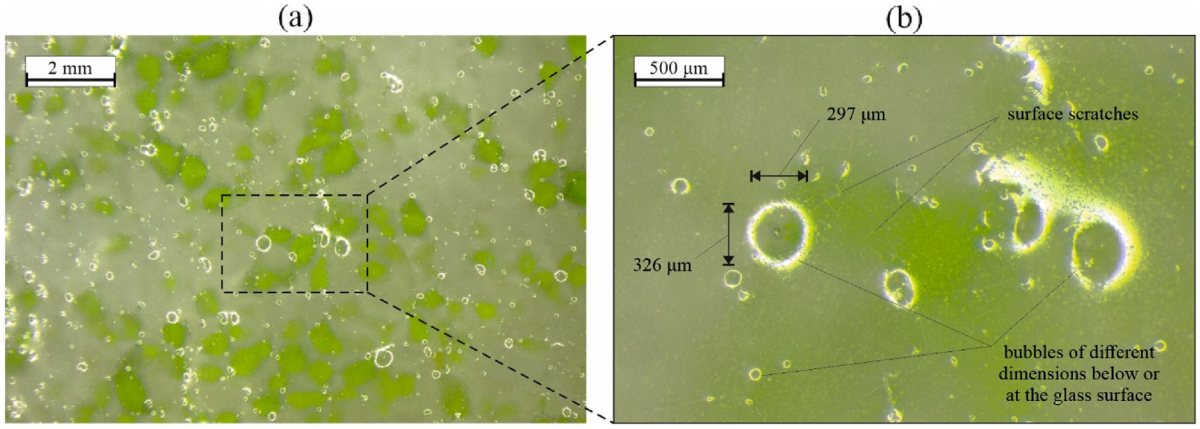

Fig. 9 Uncoloured side of kilned glass panels—representative stereo microscope images obtained with zoom factors of 10X (**a**) and 40X (**b**)

in Fig. 15a, b. Furthermore, it could be observed that the uncoloured surface was not as smooth as the reference annealed glass surfaces, exhibiting hardly visible scratches and a light texture, probably as a consequence of the textile on which the glass panels were placed during the kilning process. Figure 9b also illustrates that the kilned glass panels were not transparent anymore, but translucent, even in the areas without dispensed granules.

In the case of the coloured side of the kilned glass panels, areas with different density of dispensed and fused granules were observed. These areas seemed to exhibit variable characteristics and were therefore evaluated separately, as shown in Fig. 10. Areas with low density were considered such where only single isolated granules were observed on the glass surface (see Fig. 10a, b). Here, the different granules, which were partially immersed into the glass surface, could be clearly identified and their dimensions, which varied up to around 1 mm in diameter, could be evaluated. With the higher zoom factor of 40X, it was observed that pronounced damages of the glass surface were produced in the direct vicinity of the granules. Moreover, texturized surfaces could be identified as well in the areas without granules. Both the more pronounced damages near granules and the less pronounced texture further away from the granules could be features which lead to a decrease of the bending strength. Surface zones with different granules partially immersed in the glass surface and starting to coalesce, as those shown in Fig. 10c, d, were considered as areas with medium density. The pronounced damages around the granules started to merge in these areas, while the texturized surface parts without granules seemed to get a greenish tone and to go from translucent to opaque. Areas with high density of the dispensed and fused granules were considered such where granules could not be observed anymore as partially immersed in the glass surface, but where the entire surface was coloured with green tones and single dark-shaded green granules could be identified fully submersed in the glass (see Fig. 10e, f). With the higher zoom factor of 40X, the surface exhibited a mosaic-like texture noticeable based on the reflexions resulting through the exposure of the stereo microscope.

A detailed meaningful analysis of the fracture origins was not possible, since the acute-angled shards got chipped in these regions due to the impact of the fractured specimens to the test setup below them.

In addition to the observed modifications on the outside surface, an assessment of the depth of these modifications was made based on microscopic images of the fractured surface. The pictures in Fig. 11 show the fractured surface of a shard from a coloured kilned glass panel after completing the four-point-bending test. From Fig. 11a, illustrating areas with isolated fused granules as well as coalescing fused granules, it was observed that the granules remained near the outside surface in these areas. Figure 11b shows an isolated fused granule captured with an increased zoom factor (this granule was not situated at the fracture origin). The dimensions of such a granule were in agreement with the size range of the initially dispensed powder. It was observed that there is a fusing interface between

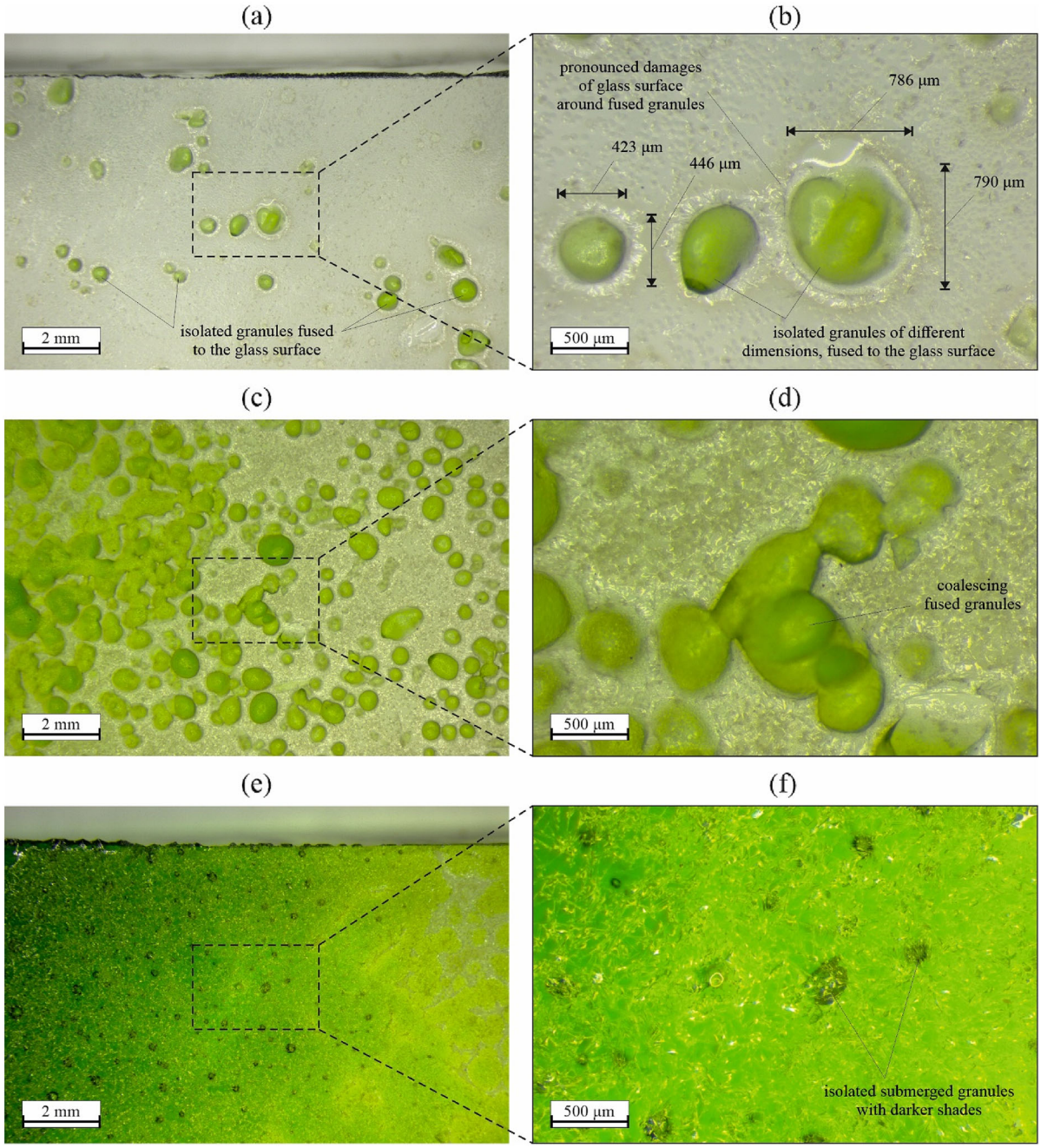

Fig. 10 Coloured side of kilned glass panels with low (**a, b**), medium (**c, d**) and high (**e, f**) density of dispensed and fused granules—representative stereo microscope images obtained with zoom factors of 10X (**a, c, e**) and 40X (**b, d, f**)

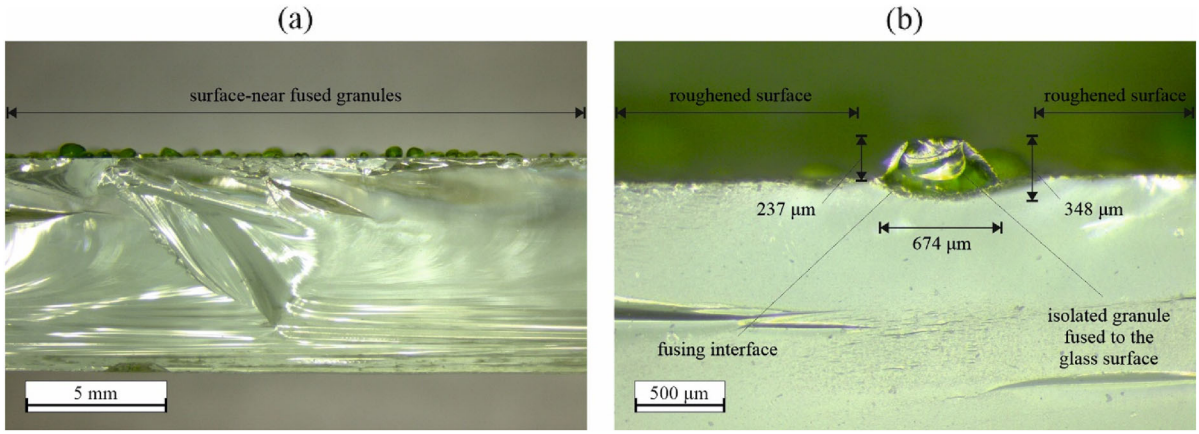

Fig. 11 Representative images obtained with the stereo microscope with zoom factors of 6.3X (**a**) and 40X (**b**) for fractured surfaces of the coloured kilned glass panels illustrating the depth to which the dispensed granules are fused into the glass surfaces

the granules and the annealed float glass surface, but no pronounce mixing was present. Furthermore, Fig. 11b shows that the glass surface on the coloured side of the kilned glass panels was not roughened only near the fused granules, but also in areas without granules. This indicated that the kilning process resulted in a texturized surface on a micro-structural level, which lead to the worse performance in the four-point-bending tests compared to the reference annealed float glass.

3.4 Analysis of surface conditions based on confocal microscope images

The surface analysis with the stereo microscope allowed for a qualitative characterization of the surface modifications generated through the production process of the coloured kilned glass. For a more precise characterisation and quantitative assessment, additional investigations based on confocal microscopy were conducted. This allowed to produce height maps of selected representative areas of the different glass surfaces and to evaluate the surface roughness along characteristic profiles. Six different glass surfaces were analysed, being (i) the air side (Fig. 12) and (ii) the tin side (Fig. 13) of the reference annealed float glass, (iii) the uncoloured side of the kilned glass (Fig. 14) and the coloured side of the kilned glass, with (iv) low (Fig. 15), (v) medium (Fig. 16) and (vi) high (Fig. 17) density of the dispensed and fused granulate. For each of these surface types, the texture was quantitatively assessed based on local features identified on 3D surface diagrams, linear waviness diagrams as well as linear roughness diagrams and average values. When comparing the results in Figs. 12, 13, 14, 15, 16 and 17 to each other, one should consider the 20 times smaller scales used in all diagrams for the reference annealed float glass. Using the same scale would have resulted in perceiving these surfaces as completely flat and smooth. This aspect also emphasized the surface texture modifications suffered by the coloured kilned glass in the production process.

The reference annealed glass exhibited similar surface characteristics both for the air side and for the tin side, as shown by Figs. 12 and 13. Singular local peaks in the 3D surface diagrams represented isolated dust particles that could not be avoided, despite carefully cleaning the surfaces before the microscopic investigations. The measured average roughness values, which were slightly higher than values found in literature (Datsiou and Overend 2016) for annealed float glass, could be attributed to the facts that (i) the glass panels were stored in exterior environment for approximately 6 months before testing and (ii) the microscopic evaluation was carried out on shard samples resulted after performing the four-point-bending tests.

When looking at the uncoloured surface of the kilned glass (see Fig. 14a, b), which was positioned on a textile material during the kilning process, different features could be noticed. The more obvious ones were the surface-near bubbles of different sizes, which were already observed with the stereo microscope and discussed in Sect. 3.3. Figure 14b highlights the surface

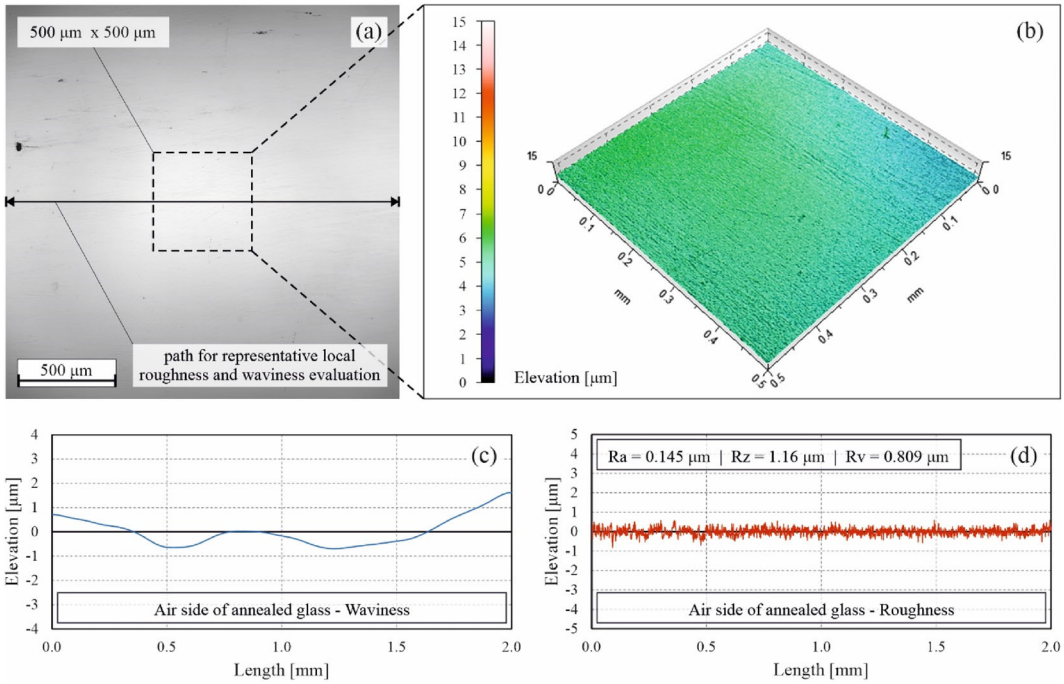

Fig. 12 Air side of the reference annealed glass panels—representative confocal microscope image (**a**), 3D surface texture (**b**), waviness profile (**c**) and roughness profile (**d**)

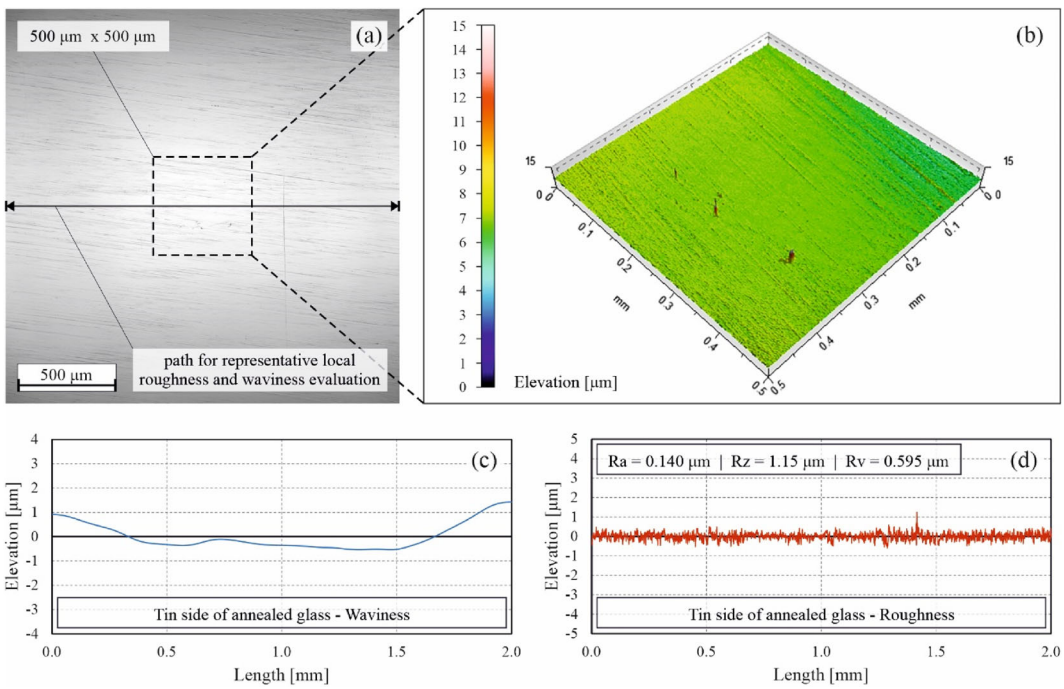

Fig. 13 Tin side of the reference annealed glass panels—representative confocal microscope image (**a**), 3D surface texture (**b**), waviness profile (**c**) and roughness profile (**d**)

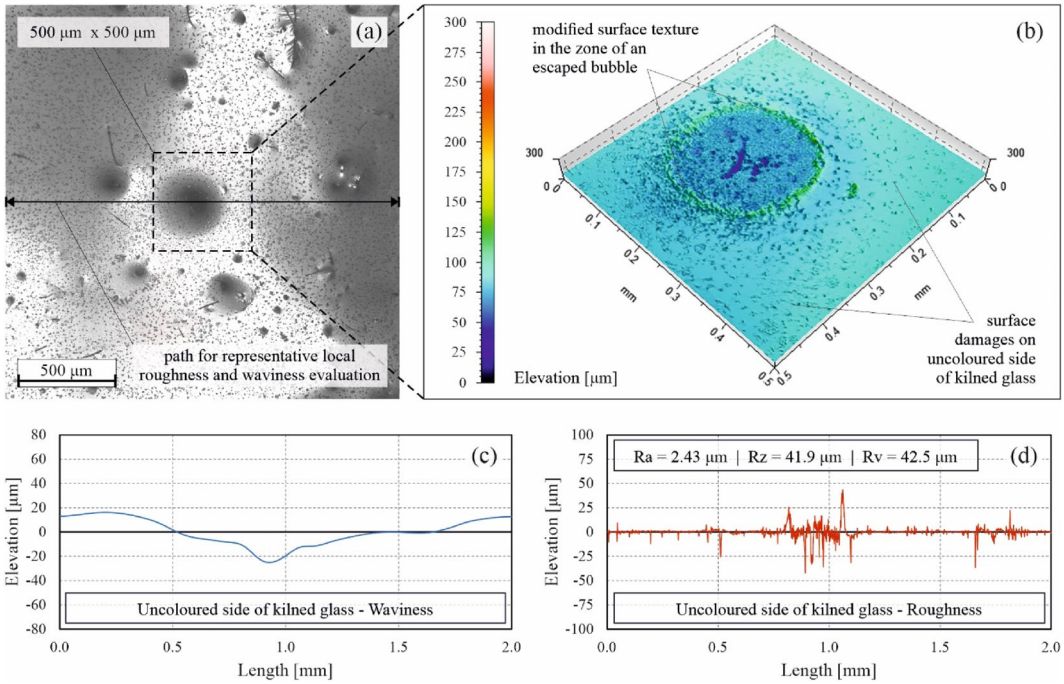

Fig. 14 Uncoloured side of kilned glass panels—representative confocal microscope image (**a**), 3D surface texture (**b**), waviness profile (**c**) and roughness profile (**d**)

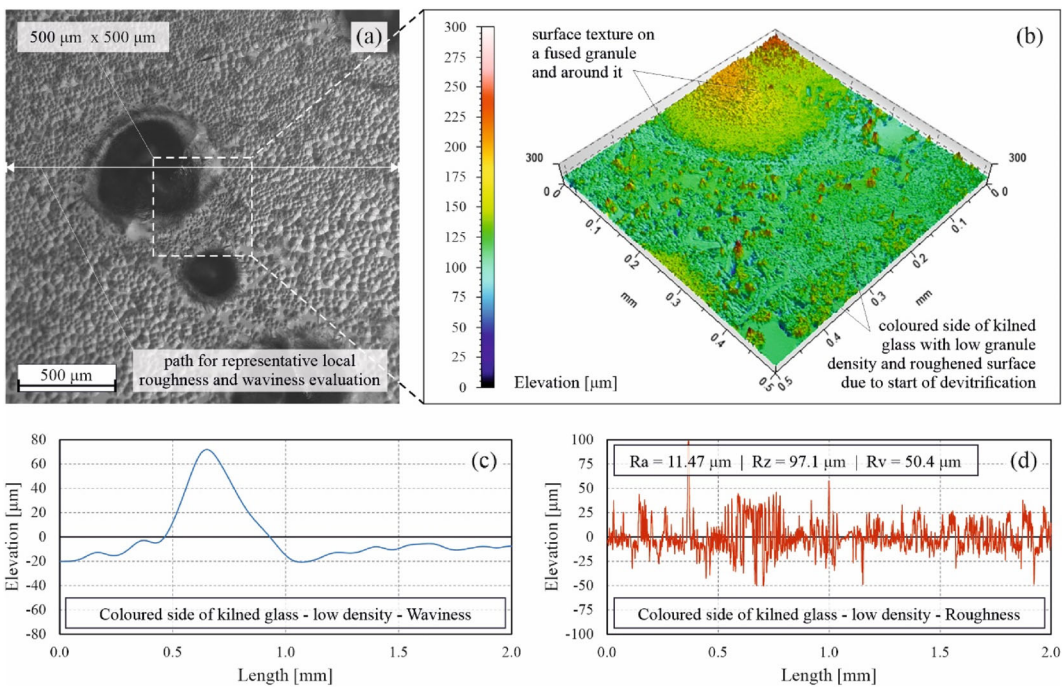

Fig. 15 Coloured side of kilned glass panels with low density of dispensed and fused granules—representative confocal microscope image (**a**), 3D surface texture (**b**), waviness profile (**c**) and roughness profile (**d**)

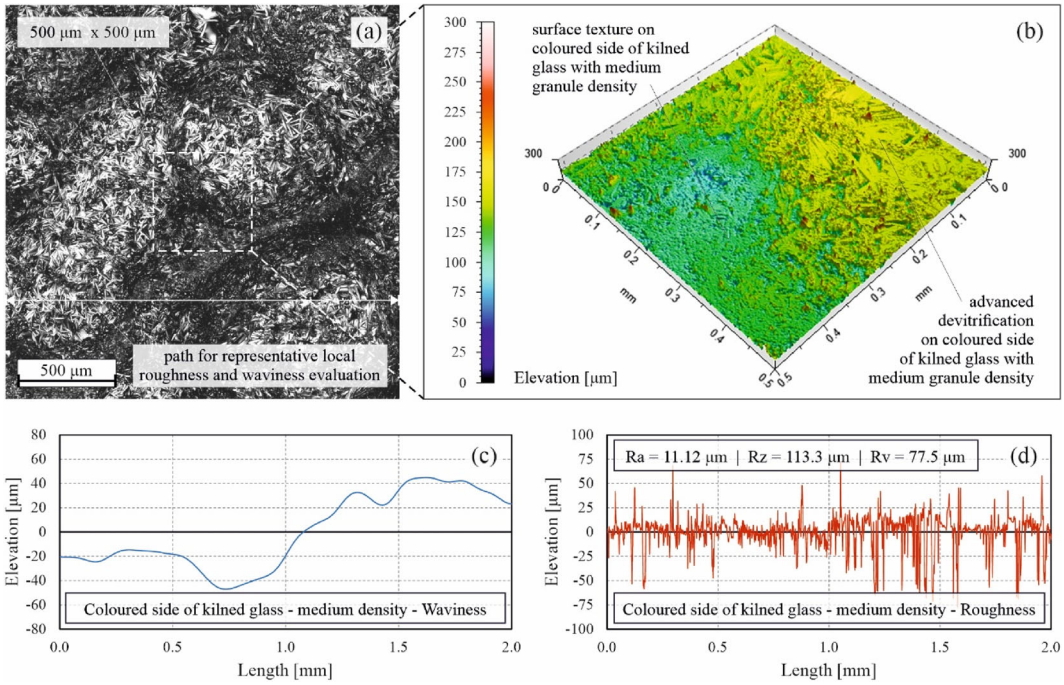

Fig. 16 Coloured side of kilned glass panels with medium density of dispensed and fused granules—representative confocal microscope image (**a**), 3D surface texture (**b**), waviness profile (**c**) and roughness profile (**d**)

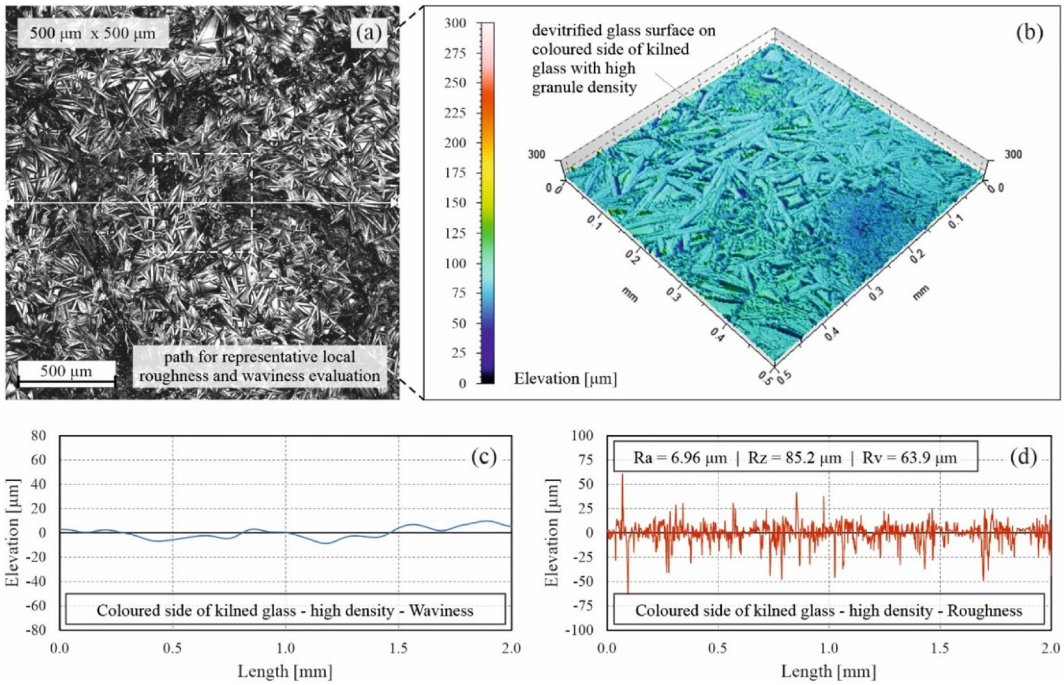

Fig. 17 Coloured side of kilned glass panels with high density of dispensed and fused granules—representative confocal microscope image (**a**), 3D surface texture (**b**), waviness profile (**c**) and roughness profile (**d**)

area where a bubble escaped the glass surface during the kilning process. In addition, some linear-shaped and some dot-shaped damages were noticed and are shown in Fig. 14a. These ones could be attributed with high probability to the textile material used below the panel. As shown by Fig. 14c, d, the uncoloured surface of the kilned glass exhibited an increased waviness and, especially in the areas around escaped bubbles, a higher roughness compared to the surfaces of the reference annealed float glass.

In case of the coloured side of the kilned glass, it was differentiated between areas with low (Fig. 15), medium (Fig. 16) and high (Fig. 17) density of the dispensed and fused granules to evaluate an eventual influence of this aspect on the quantitative surface properties. A modified texture of the surface was observed in all three cases. However, in areas with low density of granules, the granules could be clearly identified in the confocal microscopic image (see Fig. 15a), in the 3D surface diagram and in the waviness profile. In areas with medium density, only the waviness profile indicated the presence of granules, while for areas with high density, a pronounced influence of the granules on the waviness profile was not visible. In terms of roughness, the highest values were measured in areas with low density, followed closely by areas with medium density. Areas with high density of granules exhibited lower roughness values, indicating that such a distribution could be advantageous for the resulting microstructure. When looking at the surface texture in more detail, it was observed that at low granule density the glass surface exhibited an orange-skin-like pattern, while with increasing density this pattern changed more and more to a mosaic-like pattern. These aspects indicated devitrification, which can generally occur when the glass is held for too long at temperatures slightly above the softening point and can be as well boosted by dust particles present on the glass surface or in the kiln. Both of these conditions were met to a certain extent during the production process of the investigated coloured glass. A start of devitrification was observed also in areas of the kilned glass, in which no granules were deposited. The devitrification became more pronounced with higher density of deposited granules. In future investigations, the temperature curve could be varied and the kiln could be carefully cleaned for evaluating if and to what extent the devitrification process can be avoided.

The roughness values determined for the different glass surfaces, with the values for the uncoloured side of the kilned glass situated between those of the reference annealed float glass and those of the coloured side of the kilned glass, are in good agreement with the differences in structural performance observed for the different panel types in the four-point bending tests.

4 Conclusions

The results presented and discussed in this paper provided detailed insights on the structural performance and micro-structural characteristics of a novel type of coloured kilned glass panels which allows for decorative polychromatic elements. On the one hand, these findings can be used by designers to evaluate the limits of this novel type of glass and to use it in suitable applications. On the other hand, they can be a basis for a subsequent optimization of the production process with the aim of improving the structural and micro-structural properties of the coloured kilned glass panels. The following more specific conclusions can be drawn:

- The bending strength and the reachable mid-span deflection of the reference annealed float glass were reduced through the kilning and fusing processes. The magnitude of these reductions depended on whether the coloured side was under tension or compression.
- The kilning production process resulted in a more irregular geometry of the glass panels with rounded, nearly quadrant-shaped edges and uneven thickness. Especially the thinner edges influenced the fracture pattern of the kilned glass panels. The fracture initiated at the glass edge, when the coloured side was under compression and on the glass surface when the coloured side was under tension. The resulting shards had similar sizes to those of the reference annealed float glass.
- The microstructure of both the uncoloured and the coloured surfaces of the kilned glass were qualitatively modified by the production process, resulting in bending-strength-reducing features. For the coloured side, micro-structural differences were identified for areas with different density of the fused granules, ranging from surface damages around single granules to devitrification in areas with high density.
- The roughness and the waviness of the coloured kilned glass was increased by the production process. The quantitatively evaluated roughness values

were in good agreement with the different bending strength values determined from the four-point-bending test results, since the higher the local roughness of the glass surfaces subjected to tensile stresses was, the lower bending strength values were determined.

The obtained results indicate that the coloured kilned glass panels could be used in principle with similar limitations as annealed float glass or patterned glass, if the reduced strength values are considered. For a statistically significant determination of the strength value, a larger number of specimens needs to be tested. Qualitatively, the injury risk level indicated by the failure modes and the size and sharpness of the shards is similar to that of annealed float glass.

Future investigations dealing with this novel type of coloured kilned glass should on the one hand focus on studying the effects of different kilning temperature curves and support plate materials on the structural performance and micro-structural characteristics. This would allow to optimize the properties of the polychromatic glass. Furthermore, the studies should be extended to panels with diverse colour patterns to assess eventual additional effects and should include more detailed investigations of (i) the glass powder and flat glass composition (e.g. X-ray fluorescence analysis), (ii) eventual residual stresses after the fusing and kilning process for different temperature curves (e.g. analysis with polarised light) and (iii) fracture mirrors on shards without chipping. On the other hand, additional processing steps, like thermal tempering and laminating, should be assessed for the coloured kilned glass in order to allow an increased safety and a wider range of applications as façade glazing.

Acknowledgements The authors would like to gratefully acknowledge the support of the laboratory staff of the Institute of Structural Engineering at ETH Zurich in planning and manufacturing necessary parts of the four-point-bending test setup. Furthermore, the authors thank Asel Maria Aguilar Sanchez from the Institute for Building Materials and Tobias Schwarz of ScopeM for their support and assistance in obtaining the microscope images analysed in this work.

Author contributions Conceptualization: Vlad-Alexandru Silvestru; Methodology: Vlad-Alexandru Silvestru, Rena Giesecke; Formal analysis and investigation: Vlad-Alexandru Silvestru, Rena Giesecke; Writing – original draft preparation: Vlad-Alexandru Silvestru, Rena Giesecke; Writing – review and editing: Vlad-Alexandru Silvestru, Rena Giesecke, Benjamin Dillenburger; Project administration: Vlad-Alexandru Silvestru, Rena Giesecke; Supervision: Benjamin Dillenburger.

Funding Open access funding provided by Swiss Federal Institute of Technology Zurich.

Declarations

Conflict of interest On behalf of all authors, the corresponding author states that there is no conflict of interest.

References

Bristogianni, T., Oikonomopoulou, F., Yu, R., Veer, F.A., Nijsse, R.: Investigating the flexural strength of recycled cast glass. Glass Struct. Eng. **5**, 445–487 (2020). https://doi.org/10.1007/s40940-020-00138-2

Bristogianni, T., Oikonomopoulou, F., Veer, F.A.: On the flexural strength and stiffness of cast glass. Glass Struct. Eng. **6**, 147–194 (2021). https://doi.org/10.1007/s40940-021-00151-z

Datsiou, K., Overend, M.: Evaluation of artificial ageing methods for glass. In: Bos, F., Louter, C., Belis, J. (eds.) Challenging Glass 5 Conference, Ghent University (2016)

EN 1288-3: Glass in building—Determination of the bending strength of glass—Part 3: Test with specimen supported at two points (four point bending) (2000)

EN 572-1: Glass in building – Basic soda-lime silicate glass products – Part 1: Definitions and general physical and mechanical properties (2016)

EN 572-2: Glass in building—Basic soda-lime silicate glass products—Part 2: Float glass (2012)

EN 572-5: Glass in building—Basic soda-lime silicate glass products—Part 5: Patterned glass (2012)

EN ISO 4287: Geometrical Product Specifications (GPS)—Surface texture: Profile method—Terms, definitions and surface texture parameters (2010)

Giesecke, R., Dillenburger, B.: Large-scale robotic fabrication pf polychromatic relief glass. Int. J. Archit. Comput. **20**(1), 18–30 (2022). https://doi.org/10.1177/14780771221082259

Giesecke, R., Clemente, R., Mitropoulou, I., Skevaki, E., Peterhans, C.T., Dillenburger, B.: Beyond transparency, architectural application of robotically fabricated polychromatic

float glass. Constr. Robot. (2022). https://doi.org/10.1007/s41693-022-00071-6

Haldimann, M., Luible, A., Overend, M.: Structural Use of Glass. Structural Engineering document SED10. International Association for Bridge and Structural Engineering IABSE, Zurich (2008)

Inamura, C., Stern, M., Lizardo, D., Houk, P., Oxman, N.: 3D Printing and Additive manufacturing of transparent glass structures. Addit. Manuf. **5**(4), 269–283 (2018). https://doi.org/10.1089/3dp.2018.0157

Maniatis, I., Elstner, M.: Investigations on the mechanical strength of enamelled glass. Glass Struct. Eng. **1**, 277–288 (2016). https://doi.org/10.1007/s40940-016-0025-2

Oikonomopoulou, F., Bristogianni, T., Barou, L., Veer, F.A., Nijsse, R.: The potential of cast glass in structural applications Lessons learned from large-scale castings and state-of-the art load-bearing cast glass in architecture. J. Build. Eng. **20**, 213–234 (2018). https://doi.org/10.1016/j.jobe.2018.07.014

OPTUL Float: Range of granulate products. Optul Spezialglas GmbH. https://optul.de/produktpalette/granulate.html (2022). Accessed 13 June 2022

Schneider, J., Kuntsche, J., Schula, S., Schneider, F., Wörner, J.-D.: Glasbau—Grundlagen, Berechnung, Konstruktion. Springer Vieweg, Berlin (2016)

Seel, M., Akerboom, R., Knaack, U., Oechsner, M., Hof, P., Schneider, J.: Additive manufacturing of glass components—exploring the potential of glass components by fused deposition modelling. In: Louter, C., Bos, F., Belis, J., Veer, F., Nijsse, R. (eds.) Challenging Glass 6 Conference, Delft University of Technology (2018). https://doi.org/10.7480/cgc.6.2161

TNO: Glass powder printer. TNO Science and Industry. https://www.tno.nl/media/2871/hr_tno_leaflet-glasprinter.pdf (2007). Accessed 4 September 2022